BIAXIAL LOAD EFFECTS ON PLANE STRESS J-Δa- AND δ_5-Δa-CURVES

C. Dalle Donne* and H. Döker*

Results obtained from biaxial load tests on cruciform specimens with Mode I through thickness cracks and symmetrical cracks at a hole are compared with conventional crack resistance curves of compact-tension (C(T)) and center-cracked-tension (M(T)) specimens. For both of the investigated materials (Al2024-T3 and StE 460) negative loading ratios result in an increase of the uniaxially evaluated J-Δa- and δ_5-Δa-curves. Apart from one exception tension loading with $\lambda = +0.5$ seems to have no influence on the crack resistance curves. Compared to the cracked specimens the R-curves of the notched cruciformed specimens are shifted to smaller J and δ_5 values. A J-estimation formula is outlined, which takes approximately account of the load biaxiality.

INTRODUCTION

In the field of elastic-plastic fracture mechanics laboratory tests are usually carried out under uniaxial loading conditions, whereas cracks contained in actual structures experience generally a more complex loading state. The question arises whether uniaxial toughness values are transferable to biaxially loaded structures. Previous research work has been mainly concentrated on the standing crack (Liebowitz et al. (1), Miller and Kfouri (2), Alpa et al. (3), Aurich et al. (4), Turner (5) and Jansson (6)). Here the major role of biaxiality is to affect the limit load and therefore the point at which there is a rapid increase in the crack driving force expressed in terms of the applied J-integral J_{appl} or the applied crack tip opening displacement δ_{appl}. In the framework of the investigated biaxial loading ratios $-1 \leq \lambda \leq +0.5$ the work of (1), (2), (3) and (5) for a stationary crack tip and a given load F_y perpendicular to the crack can be summarized in the following way (5)

$$J_{appl}, \delta_{appl}(\lambda \leq 0) \geq J_{appl}, \delta_{appl}(\lambda = 0) \geq J_{appl}, \delta_{appl}(\lambda \geq 0) \qquad (1)$$

* German Aerospace Research Establishment (DLR), Institute of Materials Research, Cologne, Germany

The stress intensity factor of the plate with two symmetrical cracks leading off from a central hole (s. Fig. 2b) depends on the biaxial loading ratio, so that – unlike the idealized plate with a simple through crack – one finds individual J_{appl}- and δ_{appl}-loading distributions even in the elastic range. The biaxiality influences the applied crack loading parameters in the same way as the plate with a through crack when ligament yielding is reached (Kfouri (7), Amstutz and Seeger (8)).

Few experimental studies and finite element calculations on the response of crack resistance curves to biaxial loadings have been carried out (Abou-Sayed et al. (9), Garwood et al. (10), Dadkhah and Kobayashi (11) and Singh and Ramakrishnan (12)). Therefore tests with thin cruciform specimens with and without central hole (s. Fig. 2) are under way at the Institute for Materials Research of the DLR.

TEST PROCEDURE AND DATA EVALUATION

The cruciform specimens (s. Fig. 2) were machined from 6mm thick sheets of a fine grained structural steel StE 460 (Lüders yield strength σ_Y=550 N/mm^2, ultimate strength σ_U=660 N/mm^2) and of a damage tolerant aluminum alloy Al2024-T3 (σ_Y=375 N/mm^2, σ_U=491 N/mm^2). The cracks were positioned perpendicular to the plate rolling direction (LT). A uniform strain field in the centre of the specimens is achieved through the slits in the loading arms.
The tests were carried out on the servohydraulic biaxial test rig of the DLR (s. Fig. 1). The equipment has two independent loading arms with 4 load capsules, which exert up to 1000 kN in the main and up to 640 kN in the secondary axis direction. After fatigue precracking to a nominal length of a_0/W=0.3, the specimens were loaded quasistatically under displacement control.
In the case of negative loading ratios (i.e. pressure parallel to the crack) specimen buckling was prevented by anti-buckling plates that had small windows to allow accommodation of the clip gauges and of the potential probes and to contact the strain gauges on the specimens.
During the R-curve tests the following quantities were monitored by a computer (s. Fig. 2):

- Loads F_y in the main and λF_y in the secondary axis
- Crack opening displacement COD in the main loading axis
- Load line displacement V_{LL}
- Crack tip opening displacement δ_5 measured at the original fatigue crack tip (Hellmann and Schwalbe (13))
- Direct current potential drop ΔU

In the case of the notched biaxial specimen the COD measurement was taken inside the hole (s. Fig. 2b).
The amount of stable crack growth was calculated from a curve fit through the

optically identified crack lengths and the corresponding potential drops at the end of the experiments (14). In the highly ductile steel specimens the crack grew as a shear crack, whereas the crack surface of the Al2024-T3 remained virtually normal to the main loading direction and exhibited only small shear lips at the beginning of stable fracture (apart from one exception, s. below).

The J-Integral was evaluated uniaxially with the formula for M(T)-specimens reported in (13). The elastic component J_{el} was computed from the elastic stress intensity factor of the cruciform specimens (Amstutz (15)). The plastic component J_{pl} was calculated from the areas under the F_y-COD-curves, without taking account of the loading parallel to the crack. It is believed that with this procedure the influence of the biaxial loading could be shown in form of an apparent increase or decrease of the J-Δa crack resistance.
Supposing that the main effect of the loading parallel to the crack on J_{pl} is to lower or rise the plastic limit load, it is possible to derive a J_{pl}-estimation that considers load biaxiality. It was pointed out in (16) that, for ideal plasticity and constant load line displacement, J_{pl} can be written as

$$J_{pl} = -\frac{\partial A_{pl}}{2B\ \partial a} = -\frac{1}{F_{pl}}\ \frac{\partial F_{pl}}{2B\ \partial a}\ A_{pl} \tag{2}$$

where A_{pl} is the plastic component of the area under the load displacement curve and F_{pl} the plastic limit load. With a simple approximation of the limit load of the unnotched cruciform specimen (following the v. Mises criterion):

$$F_{y,pl} = \frac{2BWR_{p0.2}}{\sqrt{\lambda^2 + (1-a/W)^{-2} - \lambda\,(1-a/W)^{-1}}} \tag{3}$$

the biaxial J_λ is calculated:

$$J_\lambda = \frac{K_I^2}{E} + \frac{2-\lambda\,(1-a/W)}{2\sqrt{\lambda^2(1-a/W)^2 - \lambda\,(1-a/W)+1}}\ \frac{A_{y,pl}}{2B(W-a)} \tag{4}$$

where $A_{y,pl}$ is the plastic component under the F_y-COD curve.

RESULTS

The steel specimens fractured under large scale yielding conditions. Because of the high deformation level (especially when $\lambda<0$) these experiments had to be interrupted at a much lower amount of stable crack growth than the tests with aluminum alloy specimens, where plasticity was confined to the ligament.

Figures 3 to 6 show the crack resistance curves of the cruciform specimens with a through-thickness crack. For comparison also the crack resistance curves of centre cracked M(T) panels (W=125mm, $a_0/W=0.3$) and small C(T) specimens (W=50mm, $a_0/W=0.6$) are plotted in these diagrams.
For both materials biaxial tension loading with $\lambda=+0.5$ seems to have no influence on the J versus crack extension resistance curve, since the R-curves of the uniaxial cruciform specimen, of the $\lambda=+0.5$-loaded specimen and of the M(T)-panel lie in a common scatterband (s. Fig. 3 and 5). Compressive loading parallel to the crack leads to an apparent increase of the uniaxially determined J-R curves. Surprisingly the J-Δa-curve with $\lambda=-0.5$ lies above the curve of the steel specimens that were tested at a loading ratio $\lambda=-1$ (s. Fig. 3). This effect can also be observed in the first millimeters of stable crack growth of the aluminum biax-panels. After some amount of stable tearing the test with $\lambda=-1$ yields the highest apparent J-Δa data, probably because one of the originally flat cracks of this specimen turned into the 45°-inclined shear plane.
Figures 4 and 6 show the results of the crack tip opening measurements. The crack growth resistance in terms of δ_5 of the steel StE 460 is reduced by a tension loading parallel to the crack (s. Fig. 4) (9,10), whereas the other δ_5-Δa curves of Fig. 5 coincide at small amounts of crack extension and diverge markedly after $\Delta a \approx 3$mm. In the case of the Al2024-T3 cruciform specimens the crack tip opening resistance curves show the same dependencies as the J-Δa curves (s. Fig. 5 and 6). For this material especially the δ_5-Δa curves of the M(T) and C(T) specimens match very well (13).

The effect of load biaxiality on the resistance curves of the cruciform steel specimens with relatively short cracks emanating from a hole (s. Fig. 2b) is comparable to the influence of λ on specimens with only a through thickness crack (s. Fig. 7 and 8). Negative loading ratios result in an apparent increase of toughness, whereas $\lambda=+0.5$ reduces the δ_5-Δa curve if compared with the uniaxial loading case. The notched specimen configuration exerts a higher in-plane constraint on the crack tip than the cruciform specimen with a simple through crack (9). The crack resistance curves are thus shifted to smaller J and δ_5 values. Apart from one exception (δ_5-Δa, $\lambda=+0.5$) C(T) specimens give a conservative estimate of the crack resistance.
A compressive force parallel to the crack has practically no influence on the Al2024-T3 crack resistance curves (s. Fig. 9 and 10). The J- and δ-Δa curves correlate with the C(T)-specimen curves and the lower bound (not shown) of the M(T)-specimen scatterband.

Finally the J_λ versus stable crack growth curves are shown in the Fig. 11 and 12 (biax-panels without hole, Fig. 2a). The resistance curves of Al2024-T3 are independent of the load applied parallel to the crack, when the J-Integral is calculated with equation 4. This result is consistent with the FEM calculations of (12).

It is not possible to remove the loading ratio dependence by applying the J_λ formalism to the steel specimens (s. Fig. 11). Figure 13 displays a plot of J versus applied load for a standing crack in a steel specimen ($\lambda = -1$). The experimentally determined J-integrals using the uniaxial M(T) formula and equation 4 are compared to FEM calculations of Amstutz (15). The agreement between J_λ and the FEM calculations is not satisfactory, although J_λ gives a better estimate than the uniaxial assessed J. Further research work is under way to gain insight into these problems.

CONCLUSIONS

The present investigation of the effect of biaxial loading on stable crack growth under conditions of plane stress and fully plastic behaviour resulted in the following conclusions:

- Compressive loads parallel to the crack ($-1 \leq \lambda \leq -0.5$) lead to an apparent increase of fracture toughness expressed in terms of uniaxially evaluated J curves and to a smaller extent to an increase of the δ_5-Δa curves.
- Biaxial tension loading $\lambda = +0.5$ has no influence on R-curves (except for StE 460, δ_5-Δa).
- The effect of load biaxiality on resistance curves of notched cruciform steel specimens is comparable to the influence of biaxiality on specimens without a hole. The R-curves of notched Al2024-T3 specimen are practically not altered by a negative loading ratio.
- Because of the higher in-plane constraint of the notched configuration, the crack resistance curves of both materials are shifted to smaller J and δ_5 values.
- The resistance curves of the unnotched Al2024-T3 specimens are independent of the load applied parallel to the crack, when the J-integral is calculated with equation 4.

ACKNOWLEDGEMENTS

We gratefully acknowledge the financial support by the Deutsche Forschungsgemeinschaft (DFG). We would like to thank Mr. C. Sick and Mr. H. Frauenrath for the careful execution of the experimental work.

REFERENCES

(1) Liebowitz, H., Lee, J.D. and Eftis, J., Eng. Fract. Mech., Vol. 10, 1978, pp. 315-335.

(2) Miller, K.J. and Kfouri, A.P., ASTM STP 668, 1979, pp. 214-228.

(3) Alpa, G., Bozzo, E. and Gambarotta, L., Eng. Fract. Mech., Vol. 12,

1979, pp. 523-529.

(4) Aurich, D., Brocks, W., Jordan, R., Olschewski, J., Veith, H. and Ziebs J., "The Influence of Multiaxial Stress States on Characteristic Parameters for Cleavage Fracture in the Elastic-Plastic Range", Proc. of the AFMMS Conf., Freiburg, 1983, pp. 345-356.

(5) Turner, C.E., "Post-Yield Fracture Mechanics", Edited by D.G.H. Latzko, Elsevier Publishers, Amsterdam, 1984, pp. 25-222.

(6) Jansson, S., J. Appl. Mech., Vol. 53, 1986, pp. 555-560.

(7) Kfouri, A.P., "Elastic-Plastic FEM Analyses of Plates with Central Holes and Cracks under Biaxial Loading", EGF Publication 3, Edited by M.W. Brown and K.J. Miller, Mechanical Engineering Publications, London, 1989, pp. 25-51.

(8) Amstutz, H. and Seeger, T., "Zur Übertragbarkeit von Bruchinitiierungswerten von Standardproben auf Riß- und Lochrißscheiben unter Biax-Belastung mit Mode I Beanspruchung", 25. Sitzung des DVM-AK Bruchvorgänge", DVM Publ., Berlin, 1993, pp. 337-348.

(9) Abou-Sayed, I.S., Broek, D., Forte, T.P. and Stonesifer R.B., "Plane Stress Fracture under Biaxial Loading", Advances in Fracture Research (ICF 5), Edited by D. Francois, Pergamon Press, Oxford, 1981, Vol. 4, pp. 1707-1713.

(10) Garwood, S.J., Davey, T.G. and Creswell, S.L., Int. J. of Pres. Ves. & Piping, Vol. 36, 1989, pp. 199-224.

(11) Dadkhah, M.S. and Kobayashi, A.S., Eng. Fract. Mech., Vol. 34, 1989, pp. 253-262.

(12) Singh, R.N. and Ramakrishnan, C.V., "Biaxial Load Effects on Stable Crack Growth Using the Finite Element Method", Proc. of Third Int. Conf. Num. Meth. Fract. Mech., Swansea, 1984, pp. 261-274.

(13) Hellmann, D. and Schwalbe, K.-H., ASTM STP 833, 1984, pp. 577-605.

(14) Recommendations for Determining the Fracture Resistance of Ductile Materials, ESIS P1-90, 1990.

(15) Amstutz, H., to be published.

(16) Bucci, R.J., Paris, P.C., Landes, J.D. and Rice, J.R., ASTM STP 514, 1972, pp. 40-69.

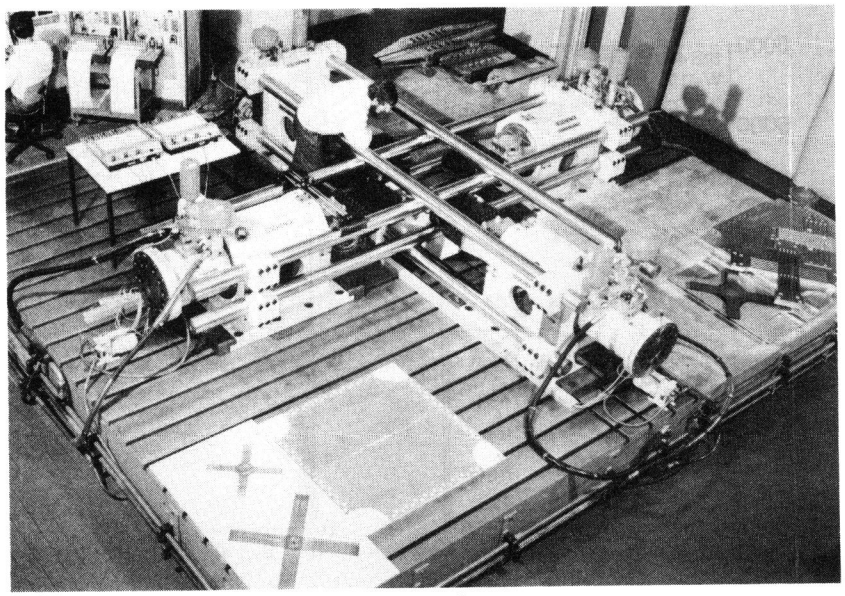

Fig. 1: Biaxial test rig with 4 load capsules

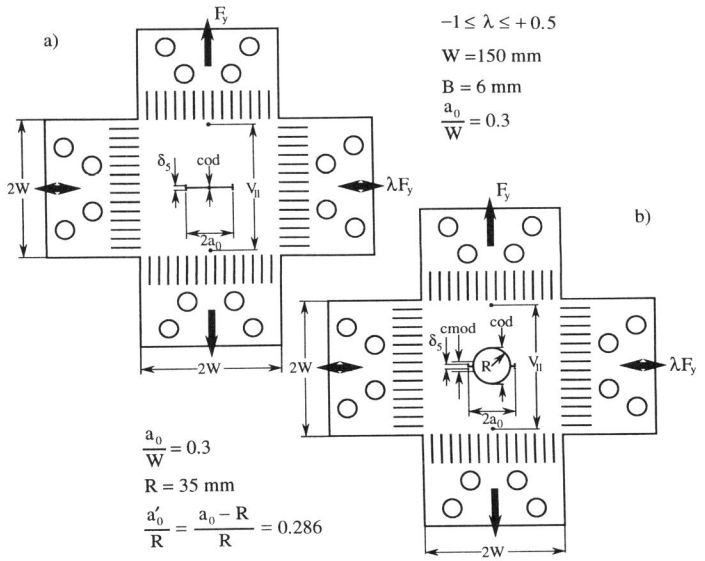

Fig. 2: Through-thickness cracked a) and notched b) cruciform specimen

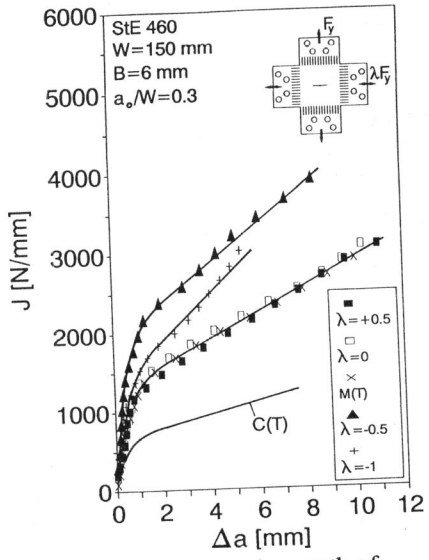

Fig. 3: J versus crack growth of steel biax-specimens (Fig. 2a)

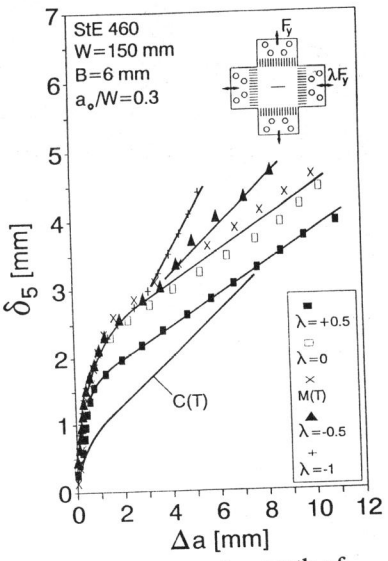

Fig. 4: δ_5 versus crack growth of steel biax-specimens (Fig. 2a)

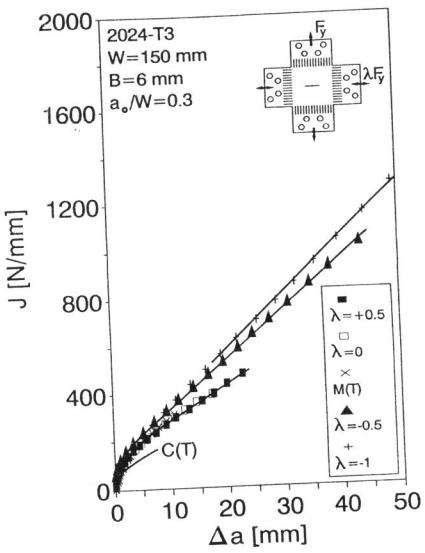

Fig. 5: J versus crack growth of Al-alloy biax-specimens (Fig. 2a)

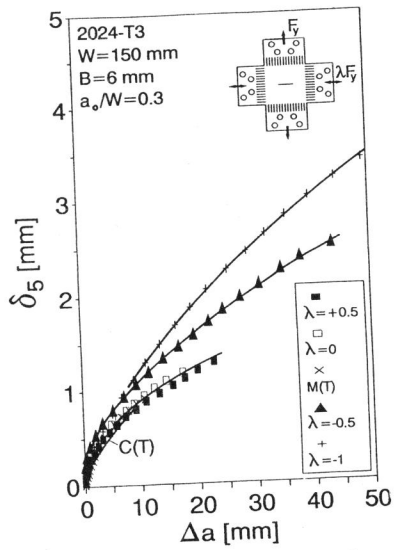

Fig. 6: δ_5 versus crack growth of Al-alloy biax-specimens (Fig. 2a)

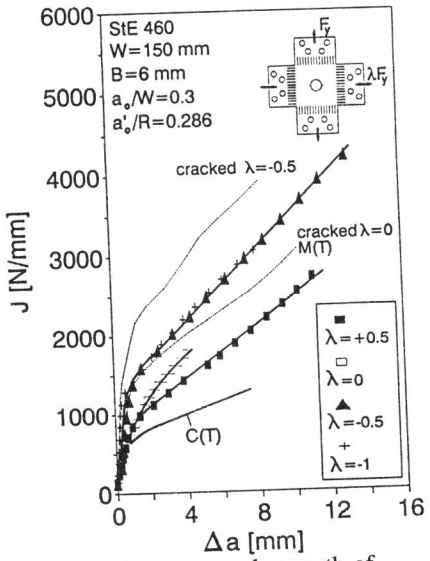

Fig. 7: J versus crack growth of notched steel specimens (Fig. 2b)

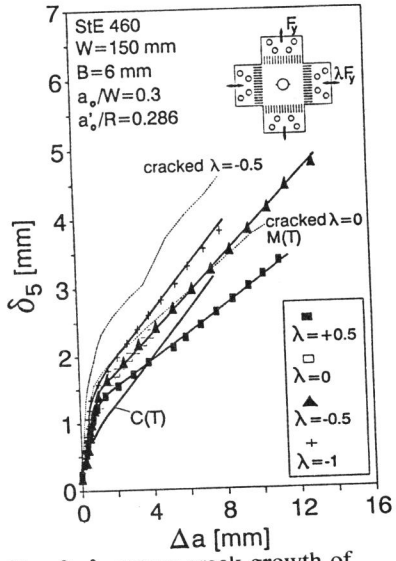

Fig. 8: δ_5 versus crack growth of notched steel specimens (Fig. 2b)

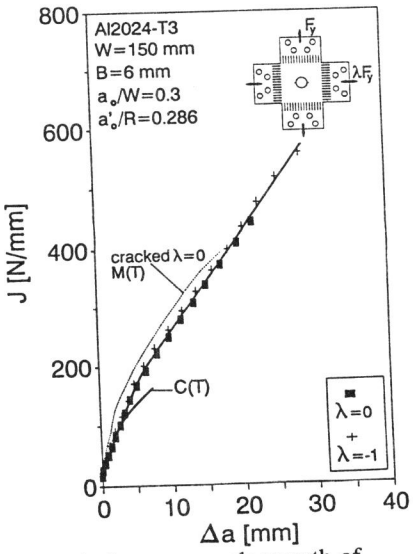

Fig. 9: J versus crack growth of notched Al-alloy specimens (Fig. 2b)

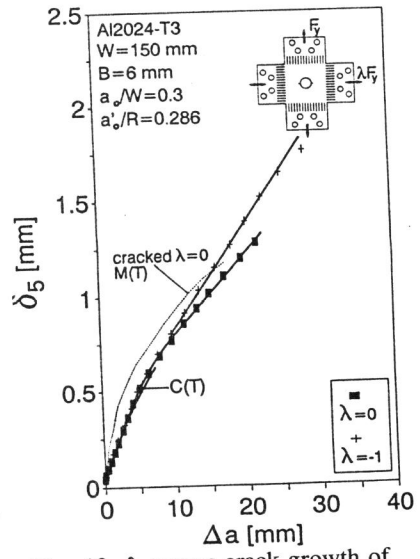

Fig. 10: δ_5 versus crack growth of notched Al-alloy specimens (Fig. 2b)

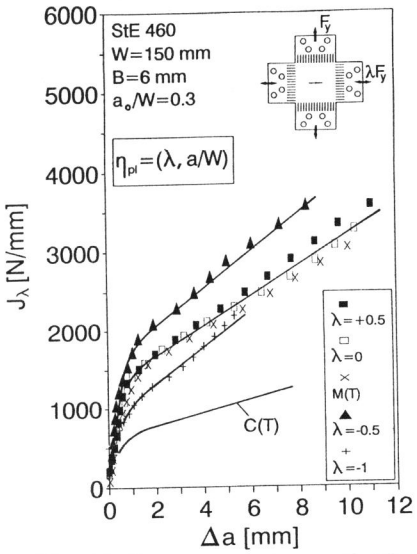

Fig. 11: J_λ versus crack growth of steel biax-specimen (Fig. 2a)

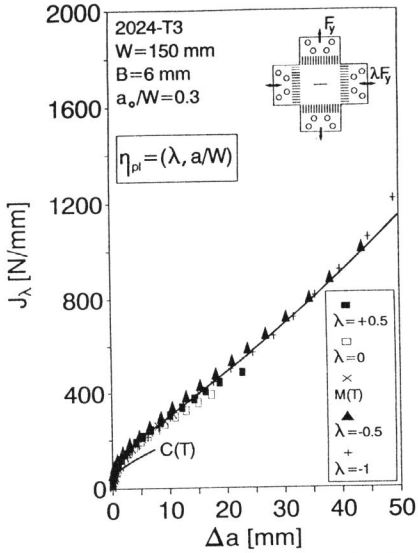

Fig. 12: J_λ versus crack growth of Al-alloy biax-specimens (Fig. 2a)

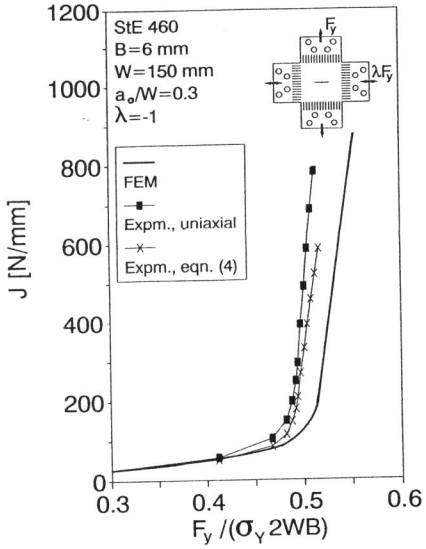

Fig. 13: Comparison of the experimentally determined J with FEM calculations of (15) (Fig. 2a)